data given in reference 20. A more detailed calculation giving similar results has been carried out by Mottelson.[21]

UNCERTAINTIES IN THE r_a DETERMINATIONS

It is evident from the model calculations indicated here that rather large unexplained effects are present in the empirical E_c values.

The $4n+1$, $4n+3$ effect amounts to as much as 250 kev of this only 150 kev have been obtained in single particle models.

From simple models including spin orbit interaction E_c breaks at subshells of $\sim$300 kev are expected the maximum observed at subshells could be $\sim$150 kev but the effect is not at all well established.

[21] B. Mottelson (private communication).

The estimate of quadrupole effects leads to a possible contribution of $\sim$100 kev to E_c. This is a rough estimate and does not take into account change in the quadrupole moment due to the added charge.

So far we have considered ground states only. In the p shell the experimental data permits an estimate of the Coulomb energy difference between the lowest $\frac{3}{2}$ and $\frac{1}{2}$ states. The results are indicated in Fig. 8, roughly speaking an effect of the order $\pm$200 kev is observed.

There is no doubt that more refined theories will explain all of these small effects, but at present I think we ought to consider them uncertainties and state that a reliable result from mirror nuclei Coulomb energies can be expressed as

$$r_0=(1.28\pm0.05)\times10^{-13}\text{ cm}.$$

REVIEWS OF MODERN PHYSICS VOLUME 30, NUMBER 2 APRIL, 1958

Nuclear Matter Distributions from Coherent Neutral Pion Production*

J. E. LEISS AND R. A. SCHRACK

National Bureau of Standards, Washington 25, D. C.

INTRODUCTION

ONE of the modes in which neutral mesons can be photoproduced from nuclei is the so-called "elastic" production in which the target nucleus recoils as a whole in its ground state. This coherent production may be used to determine nuclear radii. Since the π^0 production from neutrons and protons is essentially the same, what is measured is the distribution of nuclear matter as distinct from the electric charge distribution measured in electron scattering experiments.

Previous measurements[1–4] have shown the coherent production to be a major contribution to the photoproduction. Goldwasser[1] pointed out that in helium the elastic production has a threshold about 20 Mev lower than other modes and demonstrated that the production of π^0's in helium occurs largely in this elastic mode at low energies. Due to the high thresholds for (γ,p) and (γ,n) reactions this should also be true in carbon. Measurements at higher energies by the Massachusetts Institute of Technology group[2,3] indicate that the elastic production is still a predominant effect in photoproduction by 250 Mev photons, although the amount of inelastic production and of internal absorption of the mesons before leaving the nucleus is not clear.

It is desirable to study the coherent production in an energy region where absorption and scattering of the outgoing mesons as well as inelastic π^0 production will be small effects. This is clearly the region near the production threshold. For carbon, if we neglect the possibility of leaving the nucleus in an excited state, the energetic threshold for inelastic production is about 152 Mev compared to a threshold for elastic production of 135.6 Mev. Consideration of barrier effects, internal momentum distributions and the energy dependence of the π^0 cross section make it unlikely that the inelastic cross section will be an appreciable contribution even at 180 Mev. This supposition is borne out by this experiment.

An idea of the effects of meson absorption can be gained from Fig. 1 taken from Tenney and Tinlot.[5] This is a plot of the mean free path for absorption in nuclear matter as a function of meson energy from charged meson scattering experiments. For carbon, on which our measurements have been made, and for meson energies of less than 40 Mev, the nucleus should be quite transparent, effects due to absorption being less than 20%. We thus assume that to the accuracy of the work we are reporting, this absorption might be neglected. For a spin zero element the results of a Born

* This work supported by the U. S. Atomic Energy Commission.

[1] Goldwasser, Koester, Jr., and Mills, Phys. Rev. **95**, 1692 (L) (1954).

[2] G. De Soussure and L. S. Osborne, Phys. Rev. **99**, 843 (1955).

[3] Osborne, Barringer, Maunier, Mass. Inst. Technol. Progress Report, February 29, 1956. *Proceedings of Cern Symposium on High Energy Accelerators and Pion Physics* (June, 1956), Vol. 2, p. 282.

[4] J. E. Leiss, Bull. Am. Phys. Soc. Ser. II, **2**, 6 (1957).

[5] F. H. Tenney and J. Tinlot, Phys. Rev. **92**, 974 (1953).

approximation calculation[2,6] for elastic production from element of mass number A may be represented by Eq. (1), when we have assumed the production from neutrons and protons to be the same. The factor $F_H^2(q)$ is a form factor term added to account for the finite size of the nucleon;

$$\left[\frac{d\sigma(k)}{d\Omega}\right]_A = A^2 F_A^2(qR)\left(\frac{d\sigma(k)}{d\Omega}\right)_H \frac{1}{F_H^2(q)}. \quad (1)$$

Here k is the meson center-of-mass momentum; $F_A^2(qR)$ is the squared form factor in Born approximation for the nuclear matter distribution in element A;

$$q=\frac{1}{\hbar}(\nu^2+k^2-2\nu k\cos\theta_\pi)^{\frac{1}{2}} \quad (2)$$

is the nuclear recoil; ν is the center-of-mass photon momentum.

$[d\sigma(k)/d\Omega]_H$ is the spin independent part of the photoproduction cross section for the real proton and is related to the total spin independent cross section by

$$\left(\frac{d\sigma(k)}{d\Omega}\right)_H = \frac{3}{8\pi}\sigma_T(k)\sin^2\theta_\pi. \quad (3)$$

For a prediction of this part of the hydrogen cross section, Eq. (3), we have used the result of dispersion theory calculations by Chew *et al.*[7] kindly supplied to us by L. J. Koester. These calculations probably represent the true cross section to about 20%.

A good fit to elastic electron scattering data in carbon at 187 Mev has been obtained by Fregeau[8] using a modified gaussian charge distribution. Equation (4) is the squared modified Gaussian form factor in Born approximation divided by the squared form factor in hydrogen;

$$\frac{F_c^2(qa)}{F_H^2(q)} = \frac{\left\{\left[1-\frac{\alpha q^2a^2}{2(2+3\alpha)}\right]\exp\left(\frac{q^2a^2}{4}\right)\right\}^2}{F_H^2(q)},$$

$$\alpha=4/3,\ a=1.635\times10^{-13}\text{ cm}, \quad (4)$$

where the values of α and of a are those determined by Fregeau. The denominator of Eq. (4) is the squared form factor from electron scattering experiments in hydrogen.[9] We have assumed the same form factor for the neutron.

G. F. Chew pointed out that the form factor for hydrogen should be taken as unity. For the present experiment what is being measured is the distribution of nuclear centers in a complex nucleus. To a good approximation the ratio $F_c^2(qa)/F_H^2(q)$ as given in Eq. (4) should be used in comparing with the form factors given by electron scattering.

Figure 2 is a plot of Eq. (4) for several different incident photon energies plotted against center-of-mass meson angle, θ_π. Even at the threshold of 135.6 Mev the effect of the form factor is large, reducing the cross section by more than a factor of two. This is because the production is basically an inelastic process. For this same reason the form factor at zero degrees rises with increasing energy, approaching one when the rest energy of the meson can be neglected.

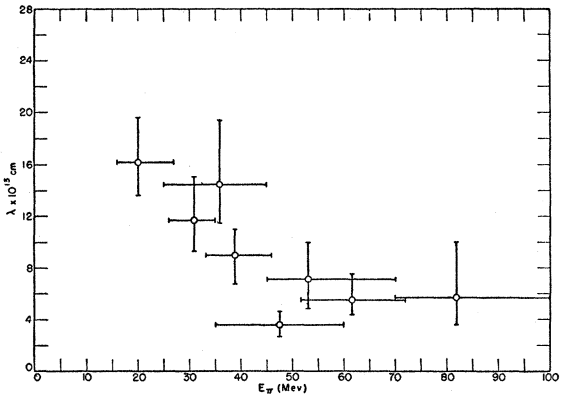

FIG. 1. Mean free path in nuclear matter for absorption of charged mesons as a function of meson energy determined from meson scattering experiments [from F. H. Tenney and J. Tinlot, Phys. Rev. **92**, 974 (1953)]. The highest meson energies in this work were about 40 Mev. The rms radius of the carbon nucleus is 2.4×10^{-13} cm (see references 8 and 9).

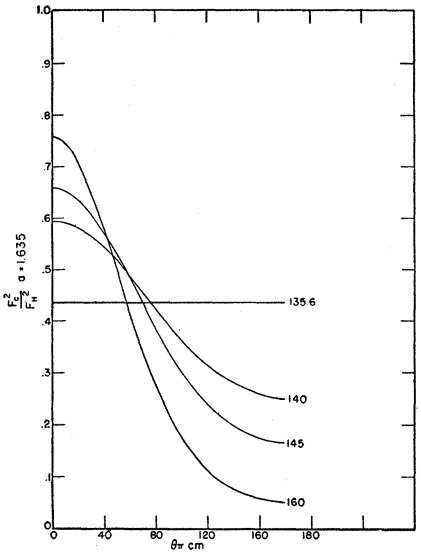

FIG. 2. Plot of the form factor from Eq. (4) as a function of π^0 angle in the center-of-mass system. The large reduction in the threshold cross section is due to the fact that the photoproduction is an inelastic process.

DESCRIPTION OF THE EXPERIMENT

The detection of π^0's is made especially difficult by their rapid decay into two photons in approximately

[6] Yoshia Yamaguchi, "Elastic production of neutral photo-pions in helium," University of Illinois report (1954).

[7] Chew, Goldberger, Low, and Nambu, Phys. Rev. **106**, 1345 (1957).

[8] Jerome H. Fregeau, Phys. Rev. **104**, 225 (1956).

[9] Robert Hofstadter, Revs. Modern Phys. **28**, 214 (1956).

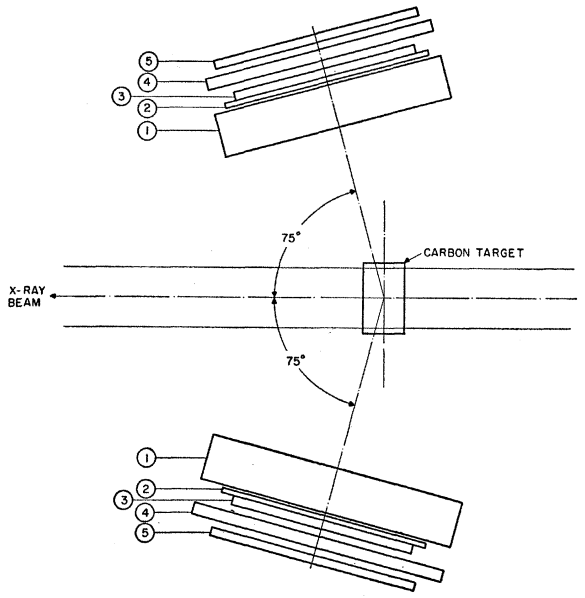

FIG. 3. Experimental arrangement of counters for the 0° case. Telescopes consist of (1) 2-in. Lucite absorbers, (2) 6.49 g/cm² lead converters, (3) 8- by 8- by ⅜-in. plastic scintillator, (4) ½-in. aluminum absorber, (5) 9- by 9- by ⅜-in. plastic scintillator.

10^{-15} seconds. This makes it mandatory to detect the decay photons rather than the π^0 itself. For this work it was decided to count the two photons in coincidence so as to reduce backgrounds and to improve the angular resolution of the detectors.

Figure 3 shows the experimental arrangement. Photons from π^0 decay are converted into pairs in the lead in front of the counters. Each pair is then detected in two plastic scintillators 8 in. and 9 in. square, respectively. Fourfold coincidences between these scintillators indicated the detection of a π^0. Many tests have indicated that the use of an anticoincidence counter is not necessary when both decay photons are detected in coincidence. The two inches of Lucite in front of the telescopes serve to prevent low-energy electron flux from reaching the counters without appreciably affecting the γ-ray detection efficiency.

Data were taken with three different positions of the counter telescopes corresponding to the plane of the counters at 0°, 90°, and 180° to the x-ray beam. Figure 3 illustrates the 0° case. The 180° case corresponds to the x-ray beam going in the opposite direction, while the 90° case corresponds to the x-ray beam perpendicular to the plane of Fig. 3. The target consisted of 7.67 g/cm² of carbon. The x-ray source was the bremsstrahlung beam from the NBS. 180 Mev synchrotron and was collimated to 6.4 cm diameter at the carbon target. For this work the synchrotron was operated so as to produce a 500-μsec yield pulse having a repetition rate of 60 pulses per second. The energy spread of this yield pulse was about 2% and was corrected for in analyzing the data.

The experimental data consisted of yield curves taken in each counter position as a function of the peak bremsstrahlung energy. Points on these yield curves were measured every 4 Mev. One of these yield curves for the counters at 90° to the x-ray beam, is shown in Fig. 4. Backgrounds of from 3 to 5 counts per hour caused by cosmic rays and accidental coincidence have been subtracted. Approximately two weeks were required to take the data shown.

Each point on Fig. 4 is the integral over the bremsstrahlung spectrum and over angle of the cross section given in Eq. (1) multiplied by the efficiency $\epsilon(\theta_\pi)$ for counting mesons produced at angles θ_π by photons of energy E. Using Eqs. (1)–(3) the points of Fig. 4 are given by

$$\gamma(E_0)=\int_0^{E_0} P(E_0,E) \times\left[(3/4)(A^2)\sigma_T{}^{(k)}\int_0^{\pi}\sin^3\theta_\pi\epsilon(\theta_\pi)\frac{F_c{}^2(\theta_\pi)}{F_H{}^2(\theta_\pi)}d\theta_\pi\right]dE, \quad (5)$$

where $P(E_0,E)$ is the bremsstrahlung spectrum of maximum energy E_0. Here the integral over azimuthal angle is absorbed into the efficiency function $\epsilon(\theta_\pi)$. The calculation of $\epsilon(\theta_\pi)$ is described in the next section. Matrix methods[10] have been developed to solve the integral Eq. (5) for an observed cross section as a function of photon energy. These techniques have been applied here, yielding an observed cross section defined by Eq. (6);

$$\sigma_{\rm obs}(k)=\tfrac{3}{4}A^2\sigma_T(k)\int_0^{\pi}\sin^3\theta_\pi\epsilon(\theta_\pi)\frac{F_c{}^2(\theta_\pi a)}{F_H{}^2(\theta_\pi)}d\theta_\pi =K(a)\sigma_T(k), \quad (6)$$

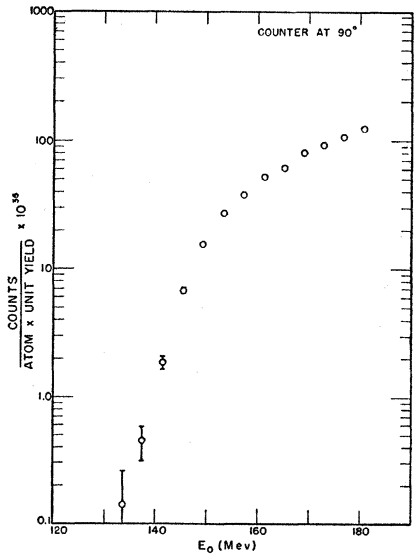

FIG. 4. Yield curve for counters at 90°. The normalization is for convenience in using cross-section analysis tables and is such as to keep the bremsstrahlung intensity constant at zero energy. Backgrounds about the size of the lowest point shown have been subtracted.

[10] A. S. Penfold and J. E. Leiss, Phys. Rev. **95**, 637(A) (1954).

where $\sigma_T(k)$ is the total spin independent cross section in hydrogen defined by Eq. (2), and a is the radius parameter defined in Eq. (4). We have explicitly set α of Eq. (4) equal to $\frac{4}{3}$ as in the elastic scattering experiments since it was not felt that a two parameter fit to the data was justified.

DETERMINATION OF THE EFFICIENCY FUNCTION $\epsilon(\theta_\pi)$

The efficiency $\epsilon(\theta_\pi)$ of the counter system for detecting π^0 decays involves two factors, the probability for the two decay γ rays to strike the two counter telescopes, and the probability of counting monoenergetic photons incident upon the counter telescopes. The second of these, the probability of detecting monoenergetic photons in one telescope was experimentally determined by a technique previously described[11] and is shown in Fig. 5 as the fraction of those photons converted into pairs by the lead converter which are actually counted. This function is believed accurate to within 10%.

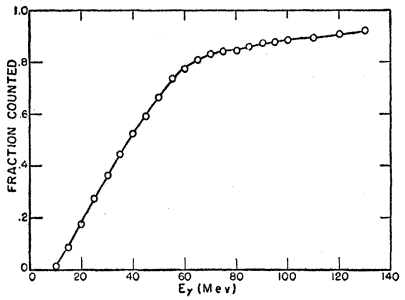

FIG. 5. Fraction of the photons converted by pair production in 6.49 gm/cm² of lead which are counted by one counter telescope in Fig. 3 plotted *versus* photon energy.

Shown in Fig. 6 is a determination of the effective size of one counter telescope measured by moving the counter telescope across a small 90-Mev x-ray beam which had previously passed through about 400 g/cm² of carbon beam hardener. The solid curve is the calculated geometrical shape. Clearly, losses resulting from edge effects in the counter telescopes are very small.

We have also rotated the telescope through this beam on a radius the same as that used in the experiment. This correctly accounts for photons striking the telescope at oblique angles. Although not quite so sharp as in Fig. 6, the error in using the geometrical size of the telescope is small.

To determine the probability of the two decay photons striking the two telescopes and being counted a Monte Carlo calculation was made on the IBM 704 computer at the National Bureau of Standards using known dynamical properties together with the data represented in Fig. 5. In this calculation the energy of the incident photon and the angle of the π^0 in the center-of-mass system was specified. The azimuthal angle around the x-ray beam was chosen at random. This meson was then allowed to decay at random in the rest system of the meson and the energy and angle of the two decay photons in the laboratory system was determined. If the two decay photons were within the two counter telescopes the probability of counting each of these photons was determined from Fig. 5 and the product of these probabilities recorded. This procedure was repeated for many different initial π^0's to get a statistically significant answer. The sizes of the target and of the x-ray beam were neglected in this calculation.

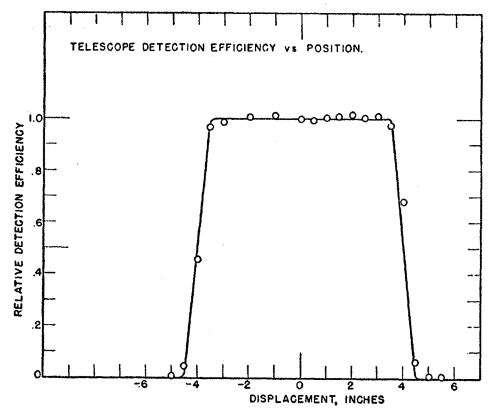

FIG. 6. Effective size of one counter telescope determined by moving telescope across a small 90-Mev, highly attenuated x-ray beam. Relative counting rate is plotted as a function of displacement across the beam. The solid curve is a calculated geometrical shape.

Figure 7 shows the results of this calculation for 160 Mev incident photons for the three different counter positions. This figure is a plot of $\sin^3\theta_\pi\epsilon(\theta_\pi)$ since as can be seen from Eq. (6) this is the weight with which the counters are affected by the form factor and is thus the quantity of greatest interest. It is interesting to note the difference between this function for the

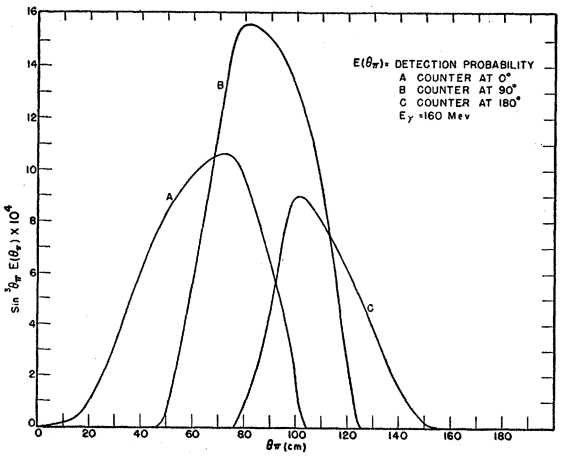

FIG. 7. Result of Monte Carlo calculation of counter efficiency for 160 Mev photons producing elastic π^0's from carbon.

[11] Leiss, Wyckoff, and Koch, Bull. Am. Phys. Soc. Ser. II, 1, 284 (1956).

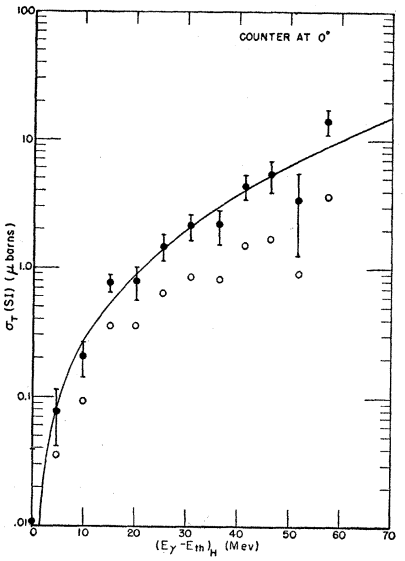

FIG. 8. Determination of total cross section for spin independent photoproduction of π^0's, $\sigma_T(SI)$, for counters at 0°. The abscissa is the photon energy in the lab system above the energetic threshold for production in hydrogen. The open circles are calculated assuming a point nucleus. The solid circles are calculated using for the radius parameter of Eq. (4), $a=1.635\times10^{-13}$ cm. Solid curve is the dispersion theory prediction of $\sigma_T(SI)$.

counters at 0° and at 180°. For an infinitely heavy nucleus those two would be the same. The fact that they are not demonstrates the rather surprising importance on the counter efficiency of the center-of-mass motion, even in an element as heavy as carbon.

For higher incident photon energies these functions become somewhat narrower, while for lower energies they become broader, until at threshold they are the same for all three counter positions except for effects of the center-of-mass motion.

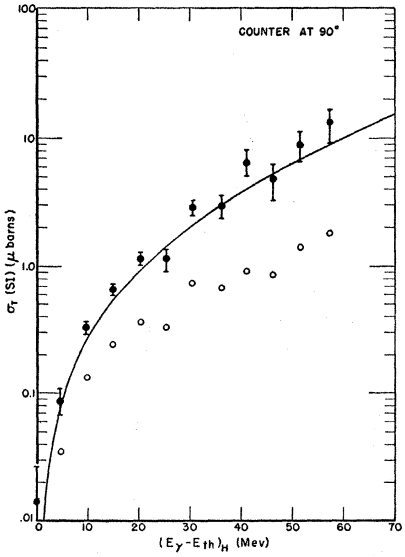

FIG. 9. Same as Fig. 8 but with the counters at 90°

REDUCTION OF THE DATA

There are two ways to represent the experimental data, first as a determination of $\sigma_T(k)$ assuming the radius is known from electron scattering experiments, and second as a determination of the radius parameter (a) assuming $\sigma_T(k)$ is known.

Equation (6) may be written as

$$\sigma_{obs}/K(a)=\sigma_T(k). \tag{7}$$

Figures 8–10 show the determination of $\sigma_T(k)$ for the three counter positions. The open circles indicate $\sigma_T(k)$ neglecting nuclear size ($a=0$). Solid circles indicate $\sigma_T(k)$ using the value $a=1.635\times10^{-13}$ cm, used by Fregeau[8] to fit electron scattering data. This fit is reasonable for all three cases although the measurement for the counters at 0° is systematically low and that for the counters at 180° systematically high. Figure 11

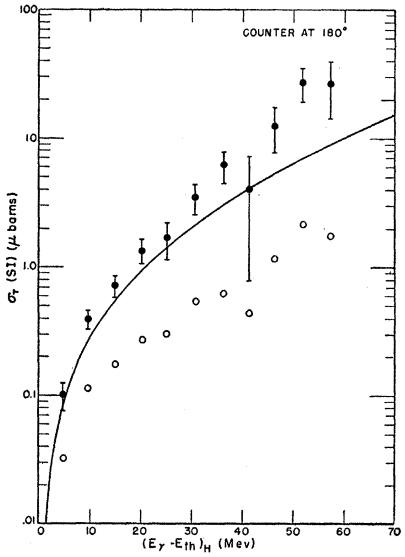

FIG. 10. Same as Fig. 8 but with the counters at 180°.

is the average of these three determinations of $\sigma_T(k)$. The solid curves in Figs. 8–11 are the dispersion theory prediction of $\sigma_T(k)$.[7]

A more sensitive plot of the data is to determine the value of the radius parameter (a) in Eq. (6) for each of the points of Figs. 8–10. This can be obtained by determining

$$\sigma_{obs}/\sigma_T(k)=K(a), \tag{8}$$

where here a is a parameter and the theoretical expression[7] is used for $\sigma_T(k)$. These determinations are shown in Fig. 12 for the three counter positions. Here the systematic variations are quite evident, the counters at 0° giving the highest value of (a) and the counters at 180° giving the lowest value. All three angles however indicate a radius close to that given by electron scattering experiments, the deviation of the average being $(1.6\pm2.8)\%$ for the counters at 0°, $(-4.6\pm1.8)\%$ for

the counters at 90° and $(-11.9\pm2.3)\%$ for the counters at 180° where the preceding errors include statistics only. The deviations correspond to a flattening of the angular distribution relative to that predicted by Eq. (1).

DISCUSSION

Within about 10% the results indicate that the average distribution of nuclear matter in C^{12} is the same as the electric charge distributions measured by electron scattering experiments. There are, however, deviations from the expected results for the different counter positions. These deviations are such as to indicate that the angular distributions are somewhat flatter than the prediction of Eq. (1).

We have attempted to find experimental effects which might explain these deviations and so far have

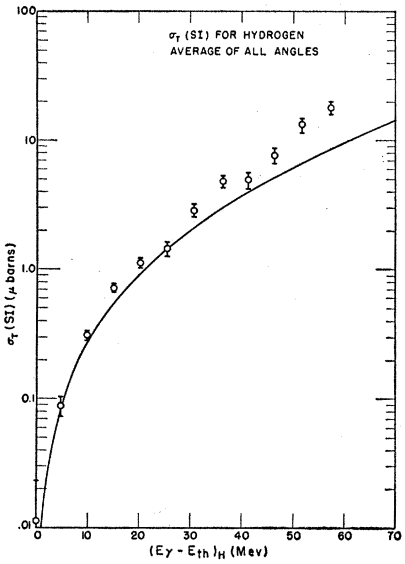

FIG. 11. Same as Fig. 8 but average of the three counter positions shown in Figs. 8–10 with $a=1.635\times10^{-13}$ cm.

been unsuccessful; however, almost any experimental effects we can think of would tend to flatten the angular distribution and thus produce deviations in the direction seen.

In Eq. (1) we have ignored the fact that the outgoing mesons travel in a complex potential well while in the nucleus. The effects of this potential have been neglected. Calculations have been made by the group at Massachusetts Institute of Technology[3] of the effects of an imaginary potential on the coherent production. Their results indicate that the angular distribution is not greatly affected by such an absorptive potential, although the normalization is changed.

We have estimated the effect of a real potential on the angular distributions. Such a potential will change both the amplitude and the phase of the various partial waves. We have considered only the phase shifts of the p and d waves and have neglected changes in the amplitudes.

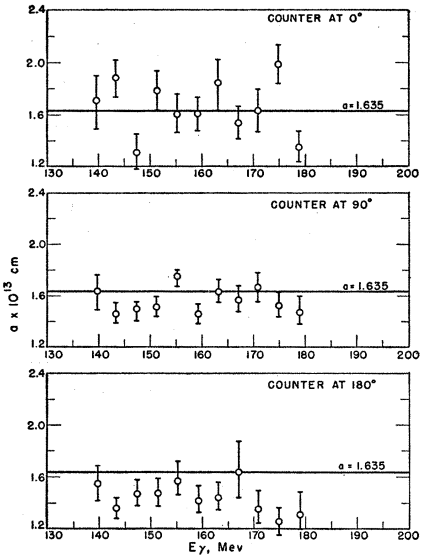

FIG. 12. Determination of the radius parameter of Eq. (4) and Eq. (8) for the three counter positions plotted *versus* laboratory photon energy. The value $a=1.635\times10^{-13}$ cm is a best fit to electron scattering experiments.

The calculation consists of performing the expansion

$$F(\theta)\sin\theta=\sum_l a_l P_l^1(\cos\theta).$$

Phase shifts in an attractive square well potential were then calculated and applied to the p and d waves of the above expression. This changes the size of the interference between the p and d waves and is in the right direction to produce the observed deviations. For a 20 Mev well which is consistent with charged meson scattering data[5] the effect is much too small however to explain the deviations seen for the counter positions used.

A change in the absolute normalization of the theoretical $\sigma_T(k)$ by as much as 30% caused either by experimental or theoretical uncertainties would change the radius determination by as much as 10%. Changes of this magnitude, however, will not remove the deviations between the three counter positions.

We plan to investigate these deviations further by measuring the coherent production in heavier elements. If the deviations are due to failure of the Born approximation there should be much larger effects in these elements.

ACKNOWLEDGMENTS

We express our appreciation to S. Penner and M. Danos for valuable discussions and active assistance during the evaluation of this work and to Alex Filipovich for long hours at the synchrotron control desk.